

See discussions, stats, and author profiles for this publication at: <https://www.researchgate.net/publication/235941958>

# Diels–Alder reactivity of butadiene and cyclic five membered dienes ((CH)<sub>4</sub>X, X=CH<sub>2</sub>, SiH<sub>2</sub>, O, NH, PH and S) with ethylene: A benchmark study

ARTICLE *in* THE JOURNAL OF PHYSICAL CHEMISTRY A · JANUARY 2002

Impact Factor: 2.69 · DOI: 10.1021/jp013910r

CITATIONS

62

READS

57

4 AUTHORS, INCLUDING:



**Tandabany C. Dinadayalane**

Clark Atlanta University

66 PUBLICATIONS 1,157 CITATIONS

SEE PROFILE



**G Narahari Sastry**

Indian Institute of Chemical Technology

262 PUBLICATIONS 5,300 CITATIONS

SEE PROFILE

# Diels–Alder Reactivity of Butadiene and Cyclic Five-Membered Dienes ((CH)<sub>4</sub>X, X = CH<sub>2</sub>, SiH<sub>2</sub>, O, NH, PH, and S) with Ethylene: A Benchmark Study

T. C. Dinadayalane, R. Vijaya, A. Smitha, and G. Narahari Sastry\*

Department of Chemistry, Pondicherry University, Pondicherry 605 014, India

Received: October 22, 2001; In Final Form: December 27, 2001

Ab initio (SCF, MP2, MP3, and CCSD(T)) and DFT (B3LYP) calculations were done on a variety of five-membered cyclic dienes, (CH)<sub>4</sub>X (X = CH<sub>2</sub>, SiH<sub>2</sub>, O, NH, PH, and S) with ethylene as a dienophile. Comparison of results with the available experimental data indicates that the CCSD(T) level with the 6-31G\* basis set is adequate in obtaining quantitative answers, both in terms of activation barriers and reaction energies. The hybrid density functional B3LYP and ab initio MP3 methods showed very good agreement with CCSD(T) results. The HF and MP2 methods are good only in reproducing the trends and fail in quantitative agreement. The changes as a function of basis set in energetics are rather small at B3LYP and MP3 levels, thus indicating that the 6-31G\* basis set is adequate to model Diels–Alder reactions. However, the dynamic electron correlation is essential in obtaining correct activation energies. The present systematic study indicates that MP3/6-31G\* is the minimum necessary level of theory to obtain reliable predictions both in terms of activation energies and in terms of reaction energies. The thermochemical data obtained at the HF method is essentially identical to that obtained at B3LYP level.

## Introduction

The synthetic utility of the Diels–Alder reaction lies in the ubiquity of a large number of dienes and dienophiles in participating in such cycloadditions.<sup>1–4</sup> The Diels–Alder reaction with the five-membered heterocyclic dienes is fundamentally interesting and is investigated in several experimental<sup>2–10</sup> and theoretical<sup>11–13</sup> studies, and this synthetic methodology provides a simple access to numerous polycyclic systems. The [4 + 2] adduct between furan (**1O**) and maleic anhydride was found to be a key intermediate in the synthesis of biologically interesting molecules<sup>3</sup> as well as polymers, such as polyelectrolytes.<sup>14,15</sup> Thiophene (**1S**) and pyrrole (**1NH**) were also found to produce useful Diels–Alder adducts, which on further refinement form basic structural frameworks for natural products and other compounds of synthetic and industrial utility.<sup>2,9,10</sup> The controversy over the mechanism of the parent reaction between butadiene and ethylene has led to a consensus, and the concerted mechanism was found to prevail over the stepwise mechanism.<sup>16–25</sup> The evidence for the synchronous concerted mechanism for the Diels–Alder reactions involving symmetric dienes and dienophiles has arrived from theoretical calculations,<sup>12f,13,18–31</sup> supported by experimental substituent effects on the rate,<sup>32</sup> deuterium kinetic isotopic effects,<sup>17,33</sup> and culminated by the elegant femtosecond experiments of Zewail et al.<sup>34</sup> However, the stepwise mechanisms could very much operate in the presence of unsymmetrical substituents especially where the substituents stabilize radical intermediates.<sup>35</sup>

Previously, the computational studies with cyclopentadiene (**1CH<sub>2</sub>**),<sup>25,27b,c,29</sup> furan (**1O**),<sup>12e,f,13</sup> thiophene (**1S**),<sup>12f,13</sup> and pyrrole (**1NH**)<sup>12d,f,13</sup> as dienes with ethylene as dienophile were performed, although the levels of computations were not uniformly high in all cases. Among the reactants considered, although silole (**1SiH<sub>2</sub>**) was unambiguously characterized in a

matrix isolation study followed by vacuum pyrolysis, its participation in the cycloaddition reaction is not explored much.<sup>36</sup> Similarly, the experimental knowledge in terms of structure and reactivity are scarce for the parent phosphole (**1PH**), whereas the substituted phosphole chemistry is well-developed.<sup>37–39</sup> To our knowledge, Diels–Alder reactions with phosphole (**1PH**) and silole (**1SiH<sub>2</sub>**) as dienes are quantitatively studied here for the first time. In this study, we concentrate only on the concerted pathway and assume that the transition states corresponding to the stepwise pathway should lie higher in energy in agreement with the previous results.<sup>20–25,28</sup>

Because good estimates of barrier heights, reaction energies, and structural and electronic features of the Diels–Alder transition states are of prime importance, we felt it is necessary to benchmark the study for the reactions of dienes depicted in Figure 1, with the ethylene taken as dienophile. With the stepwise–concerted controversy being the focal point until recently, due attention is not given to the studies aimed at assessing the suitability of the computational methodologies in modeling Diels–Alder reactions. Just around the time of settling the controversy, computational chemistry witnessed a remarkable transformation with the entry of density functional theory based calculations for studying chemical problems.<sup>40</sup> The gradient-corrected hybrid density functional theory, represented by B3LYP, with the 6-31G\* basis set was found to reproduce the experimental studies fairly well.<sup>28,29</sup> Although CASSCF methodology is taken as a good choice especially in probing the stepwise mechanisms, the energetics obtained in this procedure showed huge deviations from experimental values.<sup>21–24</sup> However, for the concerted pathway the single-determinantal procedures should be able to adequately model the potential energy surface. A perusal of the current literature reveals that computational studies ranging from semiempirical methods<sup>12,29a,41</sup> to ab initio<sup>19–27</sup> (HF, MP2, MP3, CASSCF, and CCSD(T)) and density functional theory<sup>13,25,28–31</sup> methodologies with varying

\* To whom correspondence should be addressed. E-mail: gnsastry@yahoo.com.

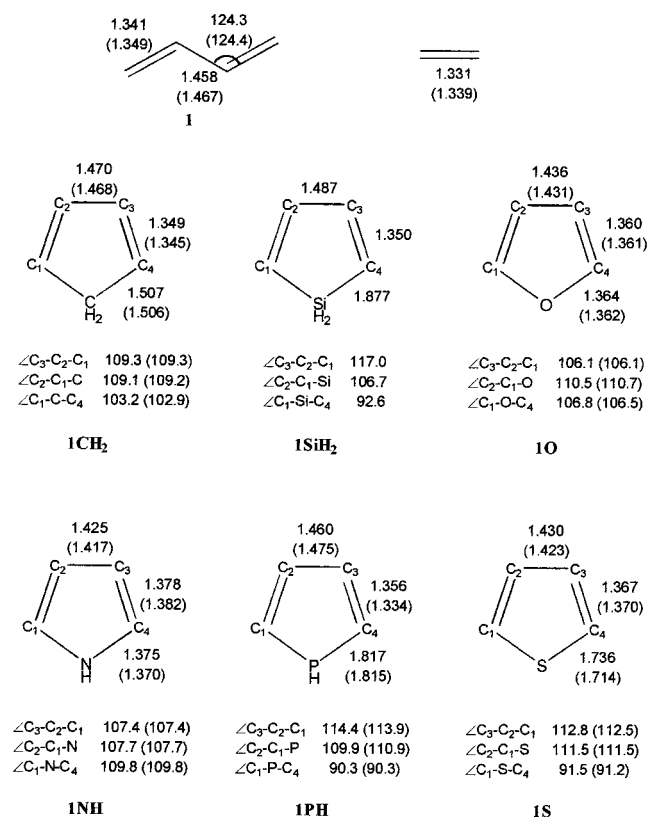


**Figure 1.** The important geometric parameters (bond lengths in Å and angles in deg) obtained at the B3LYP/6-31G\* level for all of the dienes and ethylene considered in this study. The available experimental values are given in parentheses. The experimental geometry of 1-benzylphosphole is given for phosphole (**1PH**).

basis set qualities are employed to model the potential energy profiles of the Diels–Alder reactions.

The following questions will be addressed in this study: How are the energy barriers and reaction energies affected as a function of reactant diene? How reliable are the ab initio (SCF, MP2, MP3, and CCSD(T)) and DFT methods to evaluate the energetics? What is the effect of basis set on the activation and the reaction energies? How important is the dynamic electron correlation in obtaining correct thermochemical estimates? Standard ab initio and DFT calculations are performed to answer the above questions.

## Methodology

All the ab initio and DFT calculations were done by the Gaussian 94 suite of programs.<sup>42</sup> The semiempirical AM1<sup>43</sup> and PM3<sup>44</sup> calculations were done using the MOPAC 2000 program package.<sup>45</sup> Initially, the structures of all of the reactants and products were optimized using the default gradient methods at HF, MP2, and B3LYP<sup>46</sup> levels using the 6-31G\* basis set. At the HF level, the 3-21G basis set was also used for full geometry optimizations and frequency calculations. The symmetric saddle points were located, which represent the transition states for the concerted pathway. All of the reactants and products are characterized as the minima and the saddle points as transition states by frequency calculations at HF/3-21G, HF/6-31G\*, and B3LYP/6-31G\* levels of theory as well as at semiempirical levels. A wide array of basis sets, namely, 6-31G\*, cc-pVDZ, and 6-311G\*\*, is used to assess the dependence of activation and reaction energies at the HF, MP2, MP3 and B3LYP levels of theory. Entropy of activation, reaction entropy, enthalpy of activation, and reaction enthalpy were obtained using the

B3LYP/6-31G\* frequency data, and the HF/6-31G\* computed estimates are compared. The coupled cluster method with noniterative triples correction, CCSD(T), was taken as the reference for its known excellent performance in dealing with chemical problems where the wave function is single-determinantal in nature. Although, the multideterminantal procedures are necessary for the stepwise biradicaloid pathways, single-determinantal procedures are found to be adequate for modeling the concerted pathway. Additionally, CASSCF methodology was found to grossly overestimate the activation energy and thus rendered unsuitable for quantitative energetics on the concerted pathway.<sup>21–24</sup>

## Results and Discussion

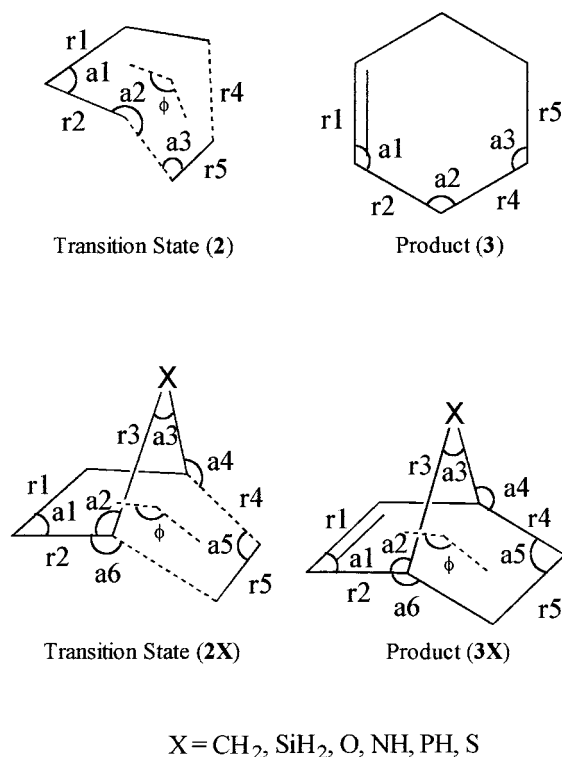
**Equilibrium Geometries.** The B3LYP/6-31G\* optimized geometries along with the experimental values, where available, of all of the reactants considered in the study are given in Figure 1. The optimized minimum energy geometries of all of the dienes are planar and possess  $C_{2v}$  symmetry except phosphole (**1PH**), where the P center is pyramidal, which results in  $C_s$  symmetry. Although the HF level gives its characteristic underestimation of the double bonds, the MP2 and B3LYP levels show excellent agreement with the experimental values (see Supporting Information). In this paper, only B3LYP/6-31G\* geometric data will be discussed from now onwards unless otherwise specified, the corresponding HF and MP2 geometric parameters are available from the accompanying Supporting Information. The reactant dienes may be classified as two categories based on the number of  $\pi$ -electrons: (a) aromatic and (b) nonaromatic. According to the recent study of Schleyer et al. the aromaticity ordering of the five-membered aromatic dienes considered in the study is as follows: pyrrole (**1NH**) > thiophene (**1S**) > furan (**1O**) > phosphole (**1PH**).<sup>47,48</sup>

All of the reactions considered in the study are assumed to follow essentially a synchronous and concerted mechanism because of the symmetry of the dienes and dienophile. Of course, in each case, the alternative stepwise biradicaloid pathway exists, which is expected to lie well over the concerted profile. The important geometric parameters of the transition states and the products are depicted in Scheme 1 and the values are given in Table 1. The synchronous saddle points are characterized as true transition states, possessing one imaginary frequency, by frequency calculations in all cases. The transition-state structures obtained for the dienes **1O** and **1NH** were tighter compared to the rest. It was recognized that the six  $\pi$ -electron delocalization near the transition state is a characteristic feature in Diels–Alder reactions.<sup>49</sup> Thus, it is expected that the bond lengths  $r_1$ ,  $r_2$ , and  $r_5$  correspond to aromatic bond length, and the equality of these three bond lengths may be taken as a measure of electron delocalization at the transition state. The comparison of bond lengths  $r_1$ ,  $r_2$ , and  $r_5$  at the transition state in Table 1 indicates that the transition states corresponding to dienes **1O**, **1NH**, and **1S** exhibit the smallest delocalization while **1** (**BD**), **1CH<sub>2</sub>**, **1SiH<sub>2</sub>**, and **1PH** show a very high delocalization. Thus, the dienes that are aromatic experience less-delocalized transition state structures, and those that are nonaromatic experience more-delocalized ones.

Syn and anti products are possible for **3PH** and **3NH**. The H attached to N or P is disposed toward the side of the plane of the diene in the syn transition state/product, whereas in the anti transition state/product, it is disposed toward the side of the incoming dienophile. In both cases, the H lies on the bisector plane of the structure. Although, both transition states could be located for **2PH**, similar attempts on **2NH** yielded only the anti

**TABLE 1: The Important Geometric Parameters of the Transition States (2 and 2X) and Products (3 and 3X) (X = CH<sub>2</sub>, SiH<sub>2</sub>, O, NH, PH, and S) Obtained at the B3LYP/6-31G\* Level<sup>a</sup>**

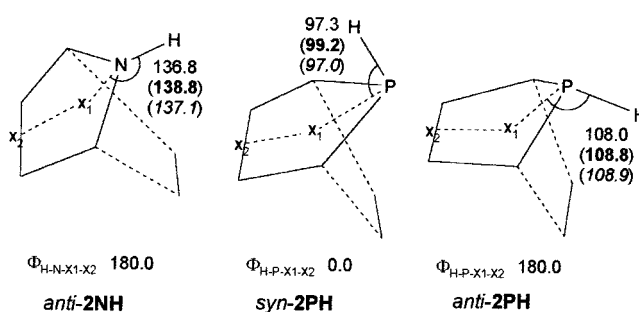
params	BD		X = CH <sub>2</sub>		X = SiH <sub>2</sub>		X = O		X = NH			X = PH				X = S	
	2	3	2CH <sub>2</sub>	3CH <sub>2</sub>	2SiH <sub>2</sub>	3SiH <sub>2</sub>	2O	3O	anti-2NH	syn-3NH	anti-3NH	syn-2PH	anti-2PH	syn-3PH	anti-3PH	2S	3S
<i>r</i> <sub>1</sub>	1.407	1.337	1.406	1.341	1.413	1.347	1.379	1.336	1.373	1.339	1.337	1.401	1.398	1.339	1.342	1.378	1.336
<i>r</i> <sub>2</sub>	1.383	1.510	1.398	1.523	1.401	1.518	1.419	1.525	1.432	1.531	1.521	1.399	1.409	1.519	1.521	1.422	1.523
<i>r</i> <sub>3</sub>			1.511	1.548	1.871	1.917	1.373	1.438	1.403	1.486	1.487	1.848	1.829	1.906	1.904	1.768	1.864
<i>r</i> <sub>4</sub>	2.272	1.537	2.248	1.568	2.253	1.568	2.150	1.565	2.126	1.564	1.574	2.249	2.242	1.568	1.560	2.182	1.561
<i>r</i> <sub>5</sub>	1.386	1.535	1.388	1.561	1.396	1.563	1.400	1.558	1.410	1.559	1.559	1.395	1.392	1.562	1.558	1.403	1.560
<i>a</i> <sub>1</sub>	122.0	123.5	109.0	107.5	115.5	112.4	105.8	105.2	106.8	106.0	106.2	113.1	112.8	110.6	110.6	111.4	109.7
<i>a</i> <sub>2</sub>	102.2	112.0	106.6	100.2	104.6	96.1	108.3	102.1	105.5	103.5	99.8	110.1	105.2	103.7	97.5	109.2	102.7
<i>a</i> <sub>3</sub>	109.1	110.0	100.0	93.6	88.8	81.5	103.3	96.0	103.4	94.6	94.5	85.2	85.9	78.4	78.6	86.1	78.7
<i>a</i> <sub>4</sub>			89.3	100.3	86.1	100.3	91.2	101.0	94.4	99.0	103.3	86.3	96.0	98.9	104.5	94.1	101.9
<i>a</i> <sub>5</sub>			101.9	102.8	105.7	107.4	100.1	100.7	100.7	101.5	101.4	104.2	104.2	105.7	105.9	103.4	105.0
<i>a</i> <sub>6</sub>			100.1	106.3	101.3	107.7	99.6	107.1	98.2	106.4	106.1	100.0	98.7	106.5	107.3	96.9	106.3
φ	118.8	180.0	105.2	111.9	111.0	118.3	103.1	111.1	102.1	111.0	110.6	107.6	106.0	114.8	116.0	103.1	113.8

<sup>a</sup> The distances and angles are given in Å and deg, respectively.**SCHEME 1**

transition structure. All attempts made toward locating the syn transition state were futile, and the putative transition state structures collapse either to products or to anti transition state upon optimization. The B3LYP/6-31G\* optimized structures of the transition states anti-2NH, along with the syn- and anti-2PH are given in Figure 2.

The percentages of bond stretching and bond shortening at the TS are evaluated and are given in Table 2. The percentage of bond alteration at the TS is calculated as the ratio of bond lengthening/shortening between the TS and the product multiplied by 100. All of these parameters help in gauging the tightness of the transition state. The calculated percentage of stretching or shortening of bonds at the TS is overestimated at the HF/6-31G\* level of theory and underestimated at the MP2/6-31G\* compared to the B3LYP/6-31G\* level. These data show that the reactions of dienes **1**, **1CH<sub>2</sub>**, **1SiH<sub>2</sub>**, and **1PH** with ethylene follow the “early” transition state where **1O**, **1NH**, and **1S** follow the “late” transition state.

**Frontier Orbital Analysis.** The synthetic viability of Diels–Alder reactions is controlled by the differential electron demand of the reactant pair. Thus, a combination of an electron-rich

**Figure 2.** The transition state structures of anti-2NH and syn- and anti-2PH obtained at the B3LYP/6-31G\* level. The angles (in deg) are given at B3LYP/6-31G\* (plain), HF/6-31G\* (bold), and MP2/6-31G\* (italics) levels.

and an electron-poor reactant pair, which ensures a reduced HOMO–LUMO gap, is predicted to witness rapid reaction.<sup>50</sup> The frontier orbital energies on the series of reactants along with the quantum of charge transfer from the diene to dienophile at the transition state geometry are given in Table 3. Both the HF/6-31G\* and B3LYP/6-31G\* levels predict identical trends except for **1**, in which case the predictions are qualitatively opposite, although the differences are marginal quantitatively. Thus, the present analysis predicts that the dienes **1CH<sub>2</sub>**, **1O**, **1NH**, and **1S** follow the normal electron demand and **1SiH<sub>2</sub>** and **1PH** follow the inverse electron demand. However, **1S** is a borderline case and the HOMO–LUMO and LUMO–HOMO interactions seem to be equally strong. The lowest frontier molecular orbital (FMO) energy gap is seen for the diene **1SiH<sub>2</sub>** at both of the levels; thus, according to FMO theory, **1SiH<sub>2</sub>** is predicted to be more reactive than the other dienes. The high reactivity of silole (**1SiH<sub>2</sub>**), particularly in cycloaddition reactions, may be traced to their elusiveness in synthetic approaches.<sup>36</sup> The reactivity ordering of dienes is predicted to be same at both of the levels. In most of the cases, the FMO energy gaps are very close. The quantum of charge transfer from the diene to the dienophile at the transition state (*q<sub>CT</sub>*) is calculated by adding the group charges of the diene portion at the transition state. Thus, a positive sign for *q<sub>CT</sub>* indicates that charge transfer occurs from the diene to the dienophile, and the negative sign corresponds to the reverse situation. The computed quantum of charge transfer from the diene to the dienophile at the transition state is in agreement with the electronic demand obtained from FMO analysis; the exception is observed in the case of **1PH** where the quantum of charge transfer at the anti-TS is predicted to be a positive value at both of the levels, and thus, the highest quantum of charge transfer is seen for the **1NH**.

**The Activation Energies.** The computed activation energies at various levels of theory are given in Table 4. Hartree–Fock–

**TABLE 2: The Percentages of Double Bonds ( $r_2$  and  $r_5$ ) Stretched and Single Bonds ( $r_1$ ) Shortened at the TS at the HF, B3LYP, and MP2 Levels with the 6-31G\* Basis Set**

system	stretching at the TS (%)						shortening at the TS (%)		
	$r_2$			$r_5$			$r_1$		
	HF	B3LYP	MP2	HF	B3LYP	MP2	HF	B3LYP	MP2
BD	29.0	24.9	22.4	31.1	27.0	24.1	51.0	42.1	39.7
X = CH <sub>2</sub>	31.4	28.2	24.5	27.1	24.8	20.7	54.8	49.6	47.0
X = SiH <sub>2</sub>	30.4	30.4	21.0	30.2	28.0	23.2	57.0	52.9	49.6
X = O	38.7	35.8	37.1	30.5	30.4	28.5	60.2	57.0	54.8
X = NH	36.5	35.3	32.8	33.3	34.7	32.6	62.3	60.5	57.7
	(38.5) <sup>a</sup>	(37.8) <sup>a</sup>	(35.2) <sup>a</sup>	(33.2) <sup>a</sup>	(34.7) <sup>a</sup>	(32.6) <sup>a</sup>	(61.1) <sup>a</sup>	(59.1) <sup>a</sup>	(56.2) <sup>a</sup>
X = PH	31.0	26.4	22.4	30.7	27.7	23.3	55.0	48.8	45.2
	(35.1) <sup>b</sup>	(32.1) <sup>b</sup>	(29.5) <sup>b</sup>	(28.3) <sup>b</sup>	(26.9) <sup>b</sup>	(23.3) <sup>b</sup>	(57.1) <sup>b</sup>	(52.5) <sup>b</sup>	(50.0) <sup>b</sup>
X = S	36.7	35.3	32.6	31.5	31.4	29.2	59.3	55.3	53.3

<sup>a</sup> The percentage of stretching or shortening of the bond calculated at the TS with respect to the total stretching/shortening of the bond at the anti product. <sup>b</sup> The percentage of stretching or shortening of the bond calculated at the anti TS.

**TABLE 3: The Frontier Orbital Energies ( $E_{\text{HOMO}}$  and  $E_{\text{LUMO}}$  in eV) of Various Dienes Considered in This Study, the FMO Energy Gap between the Dienes and Ethylene ( $E_{\text{N}}$  and  $E_{\text{I}}$  in eV), and the Quantum of Charge Transfer from Diene to Dienophile at the TS ( $q_{\text{CT}}$ )<sup>a</sup>**

diene	B3LYP/6-31G*					HF/6-31G*				
	$E_{\text{HOMO}}$	$E_{\text{LUMO}}$	$E_{\text{N}}^b$	$E_{\text{I}}^c$	$q_{\text{CT}}$	$E_{\text{HOMO}}$	$E_{\text{LUMO}}$	$E_{\text{N}}^b$	$E_{\text{I}}^c$	$q_{\text{CT}}$
<b>1</b>	-6.23	-0.61	6.74	6.65	0.000	-8.75	3.63	13.75	13.82	0.005
<b>1CH<sub>2</sub></b>	-5.76	-0.27	6.27	6.99	0.034	-8.32	3.93	13.32	14.12	0.035
<b>1SiH<sub>2</sub></b>	-6.26	-1.36	6.77	5.90	-0.013	-8.76	2.64	13.76	12.83	-0.004
<b>1O</b>	-6.11	0.54	6.62	7.80	0.053	-8.66	4.89	13.66	15.08	0.054
<b>1NH</b>	-5.48	1.39	5.99	8.65	0.104	-7.96	5.66	12.96	15.85	0.106
<b>1PH</b>	-6.25	-1.02	6.76	6.24	-0.011	-8.86	2.92	13.86	13.11	-0.013
					(0.007) <sup>d</sup>					(0.006) <sup>d</sup>
<b>1S</b>	-6.34	-0.21	6.85	7.05	0.004	-8.94	3.75	13.94	13.94	0.006

<sup>a</sup> The values are obtained at the B3LYP and HF methods with the 6-31G\* basis set. At B3LYP/6-31G\* for ethylene (dienophile),  $E_{\text{HOMO}} = -7.26$  eV and  $E_{\text{LUMO}} = 0.51$  eV. At HF/6-31G\* for ethylene (dienophile),  $E_{\text{HOMO}} = -10.19$  eV and  $E_{\text{LUMO}} = 5.00$  eV. <sup>b</sup>  $E_{\text{N}} = E_{\text{HOMO}}$  (diene) -  $E_{\text{LUMO}}$  (ethylene). <sup>c</sup>  $E_{\text{I}} = E_{\text{LUMO}}$  (diene) -  $E_{\text{HOMO}}$  (ethylene). <sup>d</sup> Quantum of charge transfer from diene to dienophile at the anti TS.

**TABLE 4: The Computed Activation Energy ( $\Delta E^\ddagger$ ) for the Diels–Alder Reactions of Butadiene (BD) and (CH)<sub>4</sub>X with Ethylene Considered in This Study at Various Levels of Theory<sup>a</sup>**

level	BD	X = CH <sub>2</sub>	X = SiH <sub>2</sub>	X = O	X = NH anti	X = PH		X = S
						syn	anti	
AM1	23.8	28.5	31.8	28.1	33.5	35.9	40.0	43.1
PM3	27.0	32.1	31.5	32.0	35.3	40.2	40.1	44.8
HF/3-21G	35.9	30.1	33.2	34.7	41.7	34.3	36.3	40.9
HF/6-31G*	45.0	39.7	41.2	42.5	47.5	44.2	44.5	52.9
	(47.7)	(42.3)						
MP2/6-31G*	17.9	11.8	11.1	18.5	22.9	15.8	15.5	26.0
	(20.3) <sup>c</sup>	(13.8) <sup>c</sup>						
B3LYP/6-31G*	22.4	19.9	19.3	25.0	30.1	24.4	24.6	34.1
	(24.8)	(22.0)						
B3LYP/cc-pVDZ <sup>b</sup>	23.6	20.9	20.8	26.3	31.7	25.7	25.8	35.4
B3LYP/6-311G** <sup>b</sup>	24.6	22.1	21.4	27.5	33.2	26.4	26.3	36.1
MP3/6-31G** <sup>b</sup>	27.2	22.7	22.8	27.2	31.4	27.2	27.3	36.5
	(29.6) <sup>c</sup>	(24.8) <sup>c</sup>						
MP3/cc-pVDZ <sup>b</sup>	26.1	21.6	21.9	26.7	30.8	26.1	26.1	35.6
MP3/6-311G** <sup>b</sup>	23.5	20.9	20.9	26.1	30.0	25.2	24.9	34.5
CCSD(T)/6-31G** <sup>b</sup>	25.1	19.8	19.8	24.7	28.3	23.6	23.9	32.7
	(27.5) <sup>c</sup>	(21.9) <sup>c</sup>						
exptl	27.5 ± 2 <sup>d</sup>	22.5 <sup>e</sup>						

<sup>a</sup> The zero-point energy corrected values are given in parentheses. All values are in kcal mol<sup>-1</sup>. <sup>b</sup> Single-point calculations were done on B3LYP/6-31G\* geometries. <sup>c</sup> Zero-point correction values are taken from frequency calculations done at B3LYP/6-31G\* level. <sup>d</sup> Taken from ref 51. <sup>e</sup> Taken from ref 52.

based methods significantly overestimate the energy barrier, and appallingly, increasing the basis set quality worsens the results (see Supporting Information). Therefore, it is very important to include dynamic electron correlation in obtaining the correct energetics. Although both MP2 and B3LYP take account of electron correlation, the way in which the electron correlation is recovered is quite different in both methods. However, the broad qualitative changes as a function of dienes and thus the trends are reproduced virtually at all levels of theory. Therefore,

while any level of theory used here is good enough for obtaining the trends in a given series, HF and MP2 are clearly unsuitable for quantitative predictions. This is in agreement with a recent study that both DFT and MP2 results show the same trends in terms of regioselectivity, stereoselectivity, and asynchronicity in a series of hetero-Diels–Alder reactions.<sup>31</sup>

In general, when the diene is more aromatic, the activation barrier for the Diels–Alder reaction is higher compared to the less aromatic and nonaromatic dienes. However, notable excep-



**TABLE 5: The Zero-Point Energy Correction ( $\Delta ZPE$ ), Enthalpy of Activation ( $\Delta H^\ddagger$ ), Entropy of Activation ( $\Delta S^\ddagger$ ), and Gibbs Free Energy of Activation ( $\Delta G^\ddagger$ ) for the Diels–Alder Reactions of Butadiene (BD) and  $(CH)_4X$  with Ethylene Considered in This Study<sup>a</sup>**

level		BD	X = CH <sub>2</sub>	X = SiH <sub>2</sub>	X = O	X = NH anti	X = PH		X = S
							syn	anti	
HF/6-31G*	$\Delta ZPE$	2.7	2.6	2.3	2.2	2.5	2.3	2.4	2.1
	$\Delta H^\ddagger$	46.2	40.8	42.1	43.3	48.6	45.2	45.5	53.7
	$\Delta S^\ddagger$	−12.6	−12.5	−12.6	−12.3	−12.5	−12.8	−12.9	−12.4
	$\Delta G^\ddagger$	58.7	53.3	54.7	55.6	61.1	58.0	58.4	66.0
B3LYP/6-31G*	$\Delta ZPE$	2.4	2.1	2.2	1.9	2.3	2.1	2.2	1.9
	$\Delta H^\ddagger$	23.4	21.0	20.3	25.7	30.0	25.3	25.5	34.8
	$\Delta S^\ddagger$	−12.1	−11.6	−12.2	−12.1	−12.3	−12.5	−12.6	−12.1
	$\Delta G^\ddagger$	35.5	(−9.6) <sup>d</sup> 32.6 (32.1) <sup>d</sup>	32.5	37.8	43.4	37.8	38.1	46.9
CCSD(T)/6-31G* <sup>b</sup>	$\Delta G^\ddagger$ <sup>c</sup>	38.2	32.4	33.0	37.5	41.5	37.0	37.4	45.5

<sup>a</sup> The available experimental values are given in parentheses. All values are in kcal mol<sup>−1</sup>. <sup>b</sup> Single point calculations on B3LYP/6-31G\* geometries. <sup>c</sup> The enthalpy and entropy correction values are obtained from the frequency calculations done at B3LYP/6-31G\* level. <sup>d</sup> Taken from ref 52.

**TABLE 6: The Computed Reaction Energy ( $\Delta E_r$ ) for the Diels–Alder Reactions of Butadiene (BD) and  $(CH)_4X$  with Ethylene Considered in This Study at Various Levels of Theory<sup>a</sup>**

level	BD	X = CH <sub>2</sub>	X = SiH <sub>2</sub>	X = O	X = NH		X = PH		X = S
					syn	anti	syn	anti	
AM1	−56.5	−27.6	−29.4	−18.0	−4.5	−4.1	−27.4	−26.1	−9.7
PM3	−52.6	−26.4	−32.4	−15.5	−10.5	−10.3	−25.0	−25.6	−8.8
HF/3-21G	−43.1	−32.0	−28.0	−16.5	−5.1	−2.0	−28.5	−29.4	−22.4
HF/6-31G*	−42.8	−24.1	−20.9	−11.7	−3.6	−1.1	−18.3	−20.7	−7.7
	(−36.0)	(−17.8)							
MP2/6-31G*	−52.5	−36.7	−37.2	−17.8	−10.6	−8.3	−31.6	−33.7	−16.0
	(−45.9) <sup>c</sup>	(−36.0) <sup>c</sup>							
B3LYP/6-31G*	−43.1	−24.4	−24.7	−8.5	−0.6	1.5	−19.3	−21.5	−6.3
	(−36.6)	(−18.4)							
B3LYP/cc-pVDZ <sup>b</sup>	−40.7	−22.4	−23.1	−5.9	2.2	4.4	−17.4	−19.4	−4.1
B3LYP/6-311G** <sup>b</sup>	−37.1	−19.0	−20.3	−3.3	5.3	7.6	−14.7	−16.7	−1.9
MP3/6-31G* <sup>b</sup>	−50.2	−32.7	−32.3	−17.9	−10.8	−8.6	−28.1	−30.1	−15.1
	(−43.8) <sup>c</sup>	(−26.7) <sup>c</sup>							
MP3/cc-pVDZ <sup>b</sup>	−48.8	−32.5	−31.5	−15.5	−9.5	−7.4	−27.5	−29.5	−14.1
MP3/6-311G** <sup>b</sup>	−51.4	−33.3	−32.5	−16.9	−10.6	−8.5	−28.6	−30.9	−15.4
CCSD(T)/6-31G* <sup>b</sup>	−46.7	−31.0	−30.2	−16.1	−9.8	−7.7	−26.4	−28.4	−13.7
	(−40.2) <sup>c</sup>	(−25.0) <sup>c</sup>							
exptl	−38.4 <sup>d</sup>	−23.2 <sup>c</sup>							

<sup>a</sup> The zero-point energy corrected values are given in parentheses. All values are in kcal mol<sup>−1</sup>. <sup>b</sup> Single-point calculations were done on B3LYP/6-31G\* geometries. <sup>c</sup> Zero-point correction values are taken from frequency calculations done at the B3LYP/6-31G\* level. <sup>d</sup> Taken from ref 53.

tions for this rule were witnessed with the reversal obtained for thiophene (**1S**) and pyrrole (**1NH**); that is, despite the higher aromaticity of pyrrole (**1NH**) over thiophene (**1S**),<sup>47,48</sup> the former was computed to exhibit greater reactivity toward cycloadditions. Table 4 indicates that the MP2 method overestimates the electron correlation and gives activation barriers that are too low.

However, the MP3 level has excellent agreement with the higher level results. Jorgensen et al. have shown that MP3/6-31G\* performs excellently in reproducing the experimental reactivity order and the enthalpies of activation in a study involving cyclopentadiene with a wide range of dienophiles.<sup>27c</sup> Thus, the conventional ab initio methods truncated at the HF and MP2 levels are found to be inapt for modeling the activation energies of Diels–Alder reactions, and MP3 seems to be a minimum requirement for obtaining quantitative answers. On the other hand, the gradient-corrected hybrid density functional method, B3LYP, has shown reasonable agreement and showed little variation as a function of the basis set. Thus, the B3LYP method with a basis set quality equal to or higher than 6-31G\* is expected to yield reliable results. The effect of basis set on the activation energy is much less at the B3LYP and MP3 levels compared to that either at the HF or at the MP2 level (see

Supporting Information). Surprisingly, semiempirical methods, especially AM1, show consistently better performance compared to the HF or MP2 levels of theory in reproducing the activation barriers for this class of compounds.

The reactivity ordering of dienes with all of the three basis sets considered at B3LYP method are as follows: **1SiH<sub>2</sub>**, **1CH<sub>2</sub>**, **1PH**, **1O**, **1NH**, and **1S**. Thus, silole (**1SiH<sub>2</sub>**) is predicted to be more reactive among all of the dienes considered in this study. The *syn*-**2PH** lies below *anti*-**2PH** by 0.2 kcal/mol at B3LYP/6-31G\*. Even though **1NH** is more aromatic than **1S**, the calculations predict that **1NH** is more reactive than **1S**.

**Thermochemical Corrections.** The computed enthalpies, entropies, and free energies of activations are given in Table 5. Earlier studies reported that B3LYP/6-31G\* enthalpy and entropy of activation parameters for the retro-Diels–Alder reaction of the norbornene are in excellent agreement with the experimental data.<sup>28</sup> To our pleasant surprise, despite the substantial differences in the computed activation barriers between HF and B3LYP, the computed thermochemical data are virtually identical in all of the cases studied here. Thus, while dynamic electron correlation is essential to obtain correct energetics, it does not seem to be necessary for obtaining the requisite thermochemical data.

**TABLE 7: The Zero-Point Energy Correction ( $\Delta ZPE$ ), Reaction Enthalpy ( $\Delta H_r$ ), Reaction Entropy ( $\Delta S_r$ ), and Gibbs Free Energy of Reaction ( $\Delta G_r$ ) for the Diels–Alder Reactions of Butadiene (BD) and (CH)<sub>4</sub>X with Ethylene Considered in This Study<sup>a</sup>**

level		BD	X = CH <sub>2</sub>	X = SiH <sub>2</sub>	X = O	X = NH		X = PH		X = S
						syn	anti	syn	anti	
HF/6-31G*	$\Delta ZPE$	6.8	6.3	5.6	5.4	6.0	5.8	6.0	6.0	5.6
	$\Delta H_r$	−38.1	−19.7	−17.0	−8.0	0.6	2.9	−14.2	−16.5	−3.8
	$\Delta S_r$	−13.8	−13.4	−13.4	−13.1	−13.3	−13.3	−13.8	−13.8	−13.2
	$\Delta G_r$	−24.3	−6.3	−3.7	5.1	13.8	16.1	−0.4	−2.7	9.4
B3LYP/6-31G*	$\Delta ZPE$	6.5	6.0	5.3	4.9	5.3	5.1	5.6	5.6	5.1
	$\Delta H_r$	−38.6	−20.3	−21.1	−5.3	2.9	4.8	−15.4	−17.6	−2.8
					(−15.2) <sup>d</sup>					
	$\Delta S_r$	−13.7	−13.3	−13.3	−13.0	−13.2	−13.2	−13.7	−13.7	−13.0
					(−10.9) <sup>d</sup>					
CCSD(T)/6-31G* <sup>b</sup>	$\Delta G_r$	−24.9	−7.0	−7.8	7.7	16.1	18.0	−1.7	−3.9	10.2
					(6.7) <sup>d</sup>					
CCSD(T)/6-31G* <sup>b</sup>	$\Delta G_r^c$	−28.5	−13.6	−13.4	0.1	6.9	8.8	−8.9	−10.8	2.8

<sup>a</sup> Experimental values are given in parentheses where available. All values are given in kcal mol<sup>−1</sup>. <sup>b</sup> Single-point calculations on B3LYP/6-31G\* geometries. <sup>c</sup> The enthalpy and entropy correction values are obtained from the frequency calculations done at the B3LYP/6-31G\* level.

<sup>d</sup> Experimental value taken from ref 3.

**Reaction Energies.** Table 6 depicts the computed reaction energies for the series of reactions considered here at various levels of theory. Unlike the activation energy data, the scatter of reaction energies is rather narrow and the trends obtained are reproduced at all of the employed levels of theory. The available experimental values are in excellent agreement with the CCSD(T) results (Table 6). In computing the reaction energies, the performance of HF and MP2 are significantly better and even comparable to B3LYP. Clearly, MP3 shows better agreement with the CCSD(T) results. Therefore, MP3 and CCSD(T) are expected to provide excellent reaction energies. Similar to the computed activation energies, the changes in the reaction energies were rather small upon increasing the quality of basis set. However, when the conventional post-HF calculations become prohibitively expensive, the hybrid density functional methods, such as B3LYP, seem to be the only viable alternative to accurately model the activation and reaction energies in this class of reactions.

The zero-point energy corrections to reaction energy, reaction enthalpies, reaction entropies, and Gibbs free energies of reactions are given in Table 7. Here also, the thermochemical data predicted at both the HF and the B3LYP level are virtually identical. The Gibbs free energies of reaction are used to discuss the feasibility of reactions. The reaction of butadiene with ethylene is more exothermic than other reactions in this study. The two products are obtained for the dienes **1NH** and **1PH**; *syn*-**3NH** is around 2 kcal mol<sup>−1</sup> lower in energy at the B3LYP/6-31G\* level than *anti*-**3NH**, whereas *syn*-**3PH** is about 2.2 kcal mol<sup>−1</sup> less stable than *anti*-**3PH** at the same level.

## Conclusions

This paper critically analyzes the performance of various computational methodologies in obtaining reliable activation and reaction energies of the Diels–Alder reaction by taking a series of five-membered dienes. The experimental values, where available, and the CCSD(T) values in other cases were taken as reference. The Diels–Alder reaction of silole (**1SiH<sub>2</sub>**) and phosphole (**1PH**) with ethylene is studied for the first time at a high level of theory. The transition states of nonaromatic dienes have more delocalization than those corresponding to the aromatic dienes. The effect of basis set on the energetics is not very significant and a basis set of 6-31G\* quality seems to be adequate in modeling this class of reactions.

The hybrid density functional B3LYP method shows excellent agreement with the CCSD(T) method and is found to be less sensitive to the changes in the basis set beyond 6-31G\* quality. The traditional HF and MP2 methods are rendered clearly unsuitable for obtaining reliable energetics. Improving the basis set quality either at HF or at MP2 level does not seem to improve the activation energy values for any reactant pair. Among the conventional ab initio methods, the MP3/6-31G\* method seems to be the minimum requirement to produce the results comparable to the B3LYP results. The thermochemical data obtained at the HF level is in good agreement with those at the B3LYP level and available experimental results. Thus, our study reinforces that the B3LYP method with the 6-31G\* basis set is not only economical but also more reliable than the HF and MP2 methodologies to model Diels–Alder reactions. In cases where performing ab initio and DFT studies are not plausible, the semiempirical AM1 method turns out to be a good alternative.

**Acknowledgment.** DST is thanked for the financial assistance. T.C.D. thanks CSIR, New Delhi, for a Junior Research Fellowship. Professor E. D. Jemmis is thanked for extending computational facilities.

**Supporting Information Available:** B3LYP/6-31G\* optimized Cartesian coordinates of all of the species considered in the study, tables of the activation and reaction energies for all of the reactions considered in the study at the HF and MP2 levels with 6-31G\*, cc-pVDZ, and 6-311G\*\* basis sets on B3LYP/6-31G\* geometries, total energies of all of the reactants, transition states, and products at various levels of theory, and the important geometric parameters of transition states and products at HF/3-21G, HF/6-31G\*, and MP2/6-31G\* levels, the figures of the important geometric parameters of reactants at HF and MP2 levels with 6-31G\* basis set, the variation of important bond lengths at TS for various dienes at B3LYP/6-31G\* level, and the correlation of activation and reaction energies for all of the Diels–Alder reactions at various levels of theory. This material is available free of charge via the Internet at <http://pubs.acs.org>.

## References and Notes

- (1) (a) Winkler, J. D. *Chem. Rev.* **1996**, *96*, 167. (b) Carruthers, W. *Cycloaddition Reactions in Organic Synthesis*; Tetrahedron Organic Chemistry Series; Pergamon Press: Elmsford, NY, 1990.

- (2) (a) Chen, Z.; Trudell, M. L. *Chem. Rev.* **1996**, 96, 1179. (b) Boger, L.; Weinberg, S. N. *Hetero Diels–Alder Methodology in Organic Synthesis*; Academic Press: New York, 1987.
- (3) Vogel, P.; Cossy, J.; Plumet, J.; Arjona, O. *Tetrahedron* **1999**, 55, 13521.
- (4) Boger, D. L. *Chem. Rev.* **1986**, 86, 781.
- (5) (a) Woodward, R. B.; Baer, H. *J. Am. Chem. Soc.* **1948**, 70, 1161. (b) Anet, F. A. L. *Tetrahedron Lett.* **1962**, 1219. (c) Lee, M. W.; Herndon, W. C. *J. Org. Chem.* **1978**, 43, 516.
- (6) Calvo-Losada, S.; Suarez, D. *J. Am. Chem. Soc.* **2000**, 122, 390.
- (7) Dewar, M. J. S.; Pierini, A. B. *J. Am. Chem. Soc.* **1984**, 106, 203.
- (8) Schmidt, R. R. *Acc. Chem. Res.* **1986**, 19, 250.
- (9) Adam, W. Delucchi, O. *Angew. Chem., Int. Ed. Engl.* **1980**, 19, 762.
- (10) (a) Jones, R. A., Ed. *The Chemistry of Heterocyclic Compounds: Pyrroles*; Wiley & Sons: New York, 1990; Vol. 48, pp 401–410. (b) Katritzky, A. R.; Rees, C. W., Eds. *Comprehensive Heterocyclic Chemistry*; John Wiley and Sons: New York, 1974; Vols. 1–8. (c) Kametani, T.; Hibino, S. *Advances in Heterocyclic Chemistry*; Academic Press: New York, 1987; Vol. 42, Chapter 2.
- (11) Avalos, M.; Babiano, R.; Bravo, J. L.; Cintas, P.; Jimenez, J. L.; Palacios, J. C.; Silva, M. A. *J. Org. Chem.* **2000**, 65, 6613.
- (12) (a) Jursic, B. S. *Tetrahedron Lett.* **1997**, 38, 1305. (b) Jursic, B. S. *J. Chem. Soc., Perkin Trans. 2* **1999**, 131. (c) Jursic, B. S. *J. Chem. Soc., Perkin Trans. 2*, **1999**, 373. (d) Jursic, B. S.; Zdravkovski, Z. *J. Mol. Struct.—THEOCHEM* **1995**, 332, 39. (e) Jursic, B. S.; Zdravkovski, Z. *J. Mol. Struct.—THEOCHEM* **1995**, 331, 215. (f) Jursic, B. S. *J. Mol. Struct.—THEOCHEM* **1998**, 454, 105. (g) Jursic, B. S. *J. Chem. Soc., Perkin Trans. 2* **1996**, 1021.
- (13) Manoharan, M.; De Proft, F.; Geerlings, P. *J. Chem. Soc., Perkin Trans. 2* **2000**, 1767.
- (14) (a) Manning, D. D.; Hu, X.; Beck, P.; Kiessling, L. L. *J. Am. Chem. Soc.* **1997**, 119, 3161. (b) Novak, B. M.; Grubbs, R. H. *J. Am. Chem. Soc.* **1988**, 110, 960.
- (15) (a) Lu, S.-Y.; Quayle, P.; Heatly, F.; Booth, C.; Yeates, S. G.; Padgett, J. C. *Macromolecules* **1992**, 25, 2692. (b) Lu, S.-Y.; Armass, J. M.; Majid, N.; Glennon, D.; Byerley, A.; Heatly, F.; Quayle, P.; Booth, C.; Yeates, S. G.; Padgett, J. C. *Macromol. Chem. Phys.* **1994**, 195, 1273.
- (16) Klarner, F.-G.; Krawczyk, B.; Ruster, V.; Deiters, U. K. *J. Am. Chem. Soc.* **1994**, 116, 7646.
- (17) Gajewski, J. J.; Peterson, K. B.; Kagel, J. R. *J. Am. Chem. Soc.* **1987**, 109, 5545.
- (18) Storer, J. W.; Raimondi, L.; Houk, K. N. *J. Am. Chem. Soc.* **1994**, 116, 9675.
- (19) Houk, K. N.; Lin, Y.-T.; Brown, F. K. *J. Am. Chem. Soc.* **1986**, 108, 554.
- (20) Bernardi, F.; Bottoni, A.; Field, M. J.; Guest, M. F.; Hiller, I. H.; Robb, M. A.; Venturini, A. *J. Am. Chem. Soc.* **1988**, 110, 3050.
- (21) Li, Y.; Houk, K. N. *J. Am. Chem. Soc.* **1993**, 115, 7478.
- (22) Sakai, S. *J. Phys. Chem. A* **2000**, 104, 922.
- (23) Wilsey, S.; Houk, K. N.; Zewail, A. H. *J. Am. Chem. Soc.* **1999**, 121, 5772.
- (24) Goldstein, E.; Beno, B.; Houk, K. N. *J. Am. Chem. Soc.* **1996**, 118, 6036.
- (25) Houk, K. N.; Beno, B. R.; Nendel, M.; Black, K.; Yoo, H. Y.; Wilsey, S.; Lee, J. K. *J. Mol. Struct.—THEOCHEM* **1997**, 398–399, 169.
- (26) Townshend, R. E.; Ramunni, G.; Segel, G.; Hehre, W. J.; Salem, L. *J. Am. Chem. Soc.* **1976**, 98, 2190.
- (27) (a) Houk, K. N.; Li, Y.; Evanseck, J. D. *Angew. Chem., Int. Ed. Engl.* **1992**, 31, 682. (b) Houk, K. N.; Loncharich, R. J.; Blake, J. F.; Jorgensen, W. L. *J. Am. Chem. Soc.* **1989**, 111, 9172. (c) Jorgensen, W. L.; Lim, D.; Blake, J. F. *J. Am. Chem. Soc.* **1993**, 115, 2936.
- (28) Beno, B. R.; Wilsey, S.; Houk, K. N. *J. Am. Chem. Soc.* **1999**, 121, 4816.
- (29) (a) Jursic, B. S. *J. Mol. Struct.—THEOCHEM* **1995**, 358, 139. (b) Jursic, B. S.; Zdravkovski, Z. *J. Chem. Soc., Perkin Trans. 2* **1995**, 1223.
- (30) Manoharan, M.; De Proft, F.; Geerlings, P. *J. Org. Chem.* **2000**, 65, 7971.
- (31) (a) Park, Y. S.; Lee, B. S.; Lee, I. *New J. Chem.* **1999**, 23, 707. (b) Park, Y. S.; Kim, W. K.; Kim, Y. B.; Lee, I. *J. Org. Chem.* **2000**, 65, 3997.
- (32) Hancock, R. A.; Wood, B. F., Jr. *J. Chem. Soc., Chem. Commun.* **1988**, 351.
- (33) Singleton, D. A.; Schulmeier, B. E.; Hang, C.; Thomas, A. A.; Leung, S.-W.; Merrigan, S. R. *Tetrahedron* **2001**, 57, 5149.
- (34) Horn, B. A.; Herek, J. L.; Zewail, A. H. *J. Am. Chem. Soc.* **1996**, 118, 8755.
- (35) Tian, J.; Houk, K. N.; Klarner, F. G. *J. Phys. Chem. A* **1998**, 102, 7662.
- (36) (a) Dubac, J.; Laporterie, A.; Manuel, G. *Chem. Rev.* **1990**, 90, 215. (b) Khabashesku, V. N.; Balaji, V.; Boganov, S. E.; Nefedov, O. M.; Michl, J. *J. Am. Chem. Soc.* **1994**, 116, 320.
- (37) Leavitt, F. C.; Manuel, T. A.; Johnson, F. *J. Am. Chem. Soc.* **1959**, 81, 3163.
- (38) (a) Coggen, P.; Engel, J. F.; Mcphail, A. T.; Quin, L. D. *J. Am. Chem. Soc.* **1970**, 92, 5779. (b) Coggen, P.; Mcphail, A. T. *J. Chem. Soc., Dalton Trans.* **1973**, 1888.
- (39) Egan, W.; Tang, R.; Zon, G.; Mislow, K. *J. Am. Chem. Soc.* **1971**, 93, 6205.
- (40) (a) Parr, R. G.; Yang, W. *Density Functional Theory of Atoms and Molecules*; Oxford University Press: New York, 1989. (b) Bartolotti, L. J.; Flurchick, K. *Rev. Comput. Chem.* **1996**, 7, 187. (c) St-Amant, A. *Rev. Comput. Chem.* **1996**, 7, 217. (d) Ziegler, T. *Chem. Rev.* **1991**, 91, 651. (e) Baerends, E. J.; Gritsenko, O. V. *J. Phys. Chem. A* **1997**, 101, 5383.
- (41) (a) Manoharan, M.; Venuvanalingam, P. *J. Phys. Org. Chem.* **1998**, 11, 133. (b) Manoharan, M.; Venuvanalingam, P. *J. Chem. Soc., Perkin Trans. 2* **1996**, 1423. (c) Manoharan, M.; Venuvanalingam, P. *J. Fluorine Chem.* **1995**, 73, 171. (d) Manoharan, M.; Venuvanalingam, P. *J. Phys. Org. Chem.* **1997**, 10, 768.
- (42) Frisch, M. J.; Trucks, G. W.; Schlegel, H. B.; Gill, P. M. W.; Johnson, B. G.; Robb, M. A.; Cheeseman, J. R.; Keith, T.; Petersson, G. A.; Montgomery, J. A.; Raghavachari, K.; Al-Laham, M. A.; Zakrzewski, V. G.; Ortiz, J. V.; Foresman, J. B.; Cioslowski, J.; Stefanov, B. B.; Nanayakkara, A.; Challacombe, M.; Peng, C. Y.; Ayala, P. Y.; Chen, W.; Wong, M. W.; Andres, J. L.; Replogle, E. S.; Gomperts, R.; Martin, R. L.; Fox, D. J.; Binkley, J. S.; Defrees, D. J.; Baker, J.; Stewart, J. P.; Head-Gordon, M.; Gonzalez, C.; Pople, J. A. *Gaussian 94*, revision D.3; Gaussian, Inc.: Pittsburgh, PA, 1995.
- (43) Dewar, M. J. S.; Zoebisch, Z.; Healy, E. F.; Stewart, J. J. P. *J. Am. Chem. Soc.* **1985**, 107, 3902.
- (44) (a) Stewart, J. J. P. *J. Comput. Chem.* **1989**, 10, 209. (b) Stewart, J. J. P. *J. Comput. Chem.* **1989**, 10, 221.
- (45) Stewart, J. J. P. *MOPAC 2000*; Fujitsu Limited: Tokyo, Japan, 1999.
- (46) (a) Becke, A. D. *J. Chem. Phys.* **1993**, 98, 5648. (b) Lee, C.; Yang, W.; Parr, R. G. *Phys. Rev. B* **1998**, 37, 785.
- (47) Schleyer, P. v. R.; Maerker, C.; Dransfeld, A.; Jiao, H.; van Eikema Hommes, N. J. R. *J. Am. Chem. Soc.* **1996**, 118, 6317.
- (48) Schleyer, P. v. R.; Freeman, P. K.; Jiao, H.; Goldfuss, B. *Angew. Chem., Int. Ed. Engl.* **1995**, 34, 337.
- (49) Evans, M. G.; Warhurst, E. *Trans. Faraday Soc.* **1938**, 34, 614.
- (50) Fleming, I. *Frontier Orbitals and Organic Chemical Reactions*; Wiley: Chichester, U.K., 1976.
- (51) Rowley, D.; Steiner, H. *Discuss. Faraday Soc.* **1951**, 10, 198.
- (52) Walsh, R.; Wells, J. M. *J. Chem. Soc., Perkin Trans. 2* **1976**, 52.
- (53) Uchiyama, M.; Tomioka, T.; Amano, A. *J. Phys. Chem.* **1964**, 68, 1878.